Journal of Multidisciplinary Engineering Science and Technology (JMEST)
ISSN: 2458-9403
Vol. 5 Issue 12, December - 2018

Analysis And Optimization Of Car Aerodynamics In Single-Phase And Two-Phase Flow Conditions With Appropriate Geometry Configuration

Charalampopoulos I. Odysseas, Grammatikopoulos S. Vasileios, Margaris P. Dionissios
Fluid Mechanics Laboratory (FML), Mechanical Engineering and Aeronautics Department
University of Patras
Patras, Greece
odysseascharalampopoulos@gmail.com, margaris@mech.upatras.gr

***Abstract*—The purpose of this paper is to analyze the aerodynamic behavior of a conventional car in conditions of heavy rainfall. The degree to which the rain impacts car's aerodynamics and ways to improve its behavior have also been investigated by applying methods of computational fluid dynamics. A CAD model of a real production car was inserted in ANSYS Fluent package in order to simulate the external flows of air and rain by using the Discrete Phase Model (DPM). Through the calculations and analysis of the flow field outside the car, we can evaluate the aerodynamic characteristics of the car (drag and lift coefficients) and proceed to optimizations through the design of aerodynamic components.**

I. INTRODUCTION

Vehicle aerodynamics analysis is crucial for car's body optimal design. Even in conventional cars and medium cruising speeds, aerodynamic drag force affects car's fuel efficiency, performance and drivability. Moreover, heavy rain may further increase the impact of drag force on car's aerodynamic behavior. Wind tunnel testing and its experimental results are the most reliable way of studying a car's aerodynamics. However, recent growth in the available computational power made the numerical simulations a very attractive choice for professionals and students. As concerns the external flows (such as the relative movement of a car to air) Computational Fluid Dynamics (CFD) methods aid the analysis of the flow field around an object without creating a physical model, leading to reduced time and cost of research projects. In order to study the one phase flow of air and the two phase flow of air/water in form of rain, around the car's body, a detailed CAD model was created and CFD analysis was applied in ANSYS Fluent. The prediction of boundary layer separation, areas of high pressure gradients and reverse flow regions are of high concern as they compose the main causes of aerodynamic drag.

Aim of this paper is to improvise the aerodynamic behavior of a car by increasing the total downforce generated by the car's body in conditions of steady airflow and rain at velocities of 100 and 140 km/h. A NACA-type airfoil was designed in Solidworks and added to the back of the car. Then, simulations before and after the addition of the airfoil were resolved in both velocities and their results were visualized in order to obtain accurate aspect of the flow. Drag and lift coefficients were the basic aerodynamic characteristics which were studied.

II. CFD ANALYSIS ON VEHICLE GEOMETRY

A. The Navier Stokes governing equations

The flow field is analyzed by numerical methods so motion and trajectories of involving fluid flows particles are predicted. The software's solver uses an iterative procedure for calculating the properties of the flow while in every following iteration the accuracy of the solution is increased. The governing equations which describe the motion and physics of fluids are known as Navier Stokes equations. Mass, momentum and heat transfer are calculated in all three dimensions for each point of the domain. Although the process of solving these equations is complicated, with the appropriate assumptions we can model a fluid flow with sufficient accuracy by using a CFD package.

Below, Navier-Stokes equations are presented in their scaled form for a Cartesian coordinate system. Eq. (1) is the continuity equation and Eq. (2) are the momentum equations. [1]

$$\frac{d}{dt}(\rho)+\frac{d}{dx}(\rho u)+\frac{d}{dy}(\rho v)+\frac{d}{dz}(\rho w)=0 \tag{1}$$

$$\frac{d}{dt}(\rho u)+\frac{d}{dx}(\rho u^2+p-\tau_{xx})+\frac{d}{dy}(\rho uv-\tau_{yx})+\frac{d}{dz}(\rho uw-\tau_{zx})-\rho g_x=0$$

$$\frac{d}{dt}(\rho v)+\frac{d}{dx}(\rho uv-\tau_{yx})+\frac{d}{dy}(\rho v^2+p-\tau_{yy})+\frac{d}{dz}(\rho uw-\tau_{zy})-\rho g_y=0$$

$$\frac{d}{dt}(\rho w)+\frac{d}{dx}(\rho uw-\tau_{zx})+\frac{d}{dy}(\rho wv-\tau_{yz})+\frac{d}{dz}(\rho w^2+p-\tau_{zz})-\rho g_z=0 \tag{2}$$

In the equations above, the mean values of each variable is replaced. For example the density:

$$\rho=\bar{\rho}+\rho' \tag{3}$$

B. Boundary layer and RANS models

The flow is composed of three main regimes. The laminar regime, the transitional and the turbulent. As long as the fluid remains in the laminar regime (low Reynolds numbers) we can solve the steady – state Navier – Stokes equations. However, in the other two regimes and as the fluid's behavior starts presenting large eddies in small time lapses, it is computationally unfeasible to predict the actual flow motion at each time [2]. At this point a Reynolds Averaged Navier Stokes (RANS) approach of the physical problem is selected. These equations do not solve the small fluctuations of the flow but instead, they approximate them numerically and model them with turbulent mathematical models. The turbulent flow is characterized by random fluctuations of physical magnitudes within the flow field. In order to be solved numerically, the quantities are divided into average values in the time domain.

Even in turbulent flows that are fully developed, inside the boundary layer three regions steal exist. The viscous sublayer and the transitional layer are playing an important role in flow's modelling. In case of external flows with high Reynold numbers the prediction of detachment and reattachment of the boundary layer, the separating points and the physical mechanisms of the fluid that take place inside the viscous sublayer are high importance matters.

C. Turbulence models

In order to model the turbulent flow, ANSYS Fluent supplies a variety of turbulence models. In the present paper, we have some default restrictions for which models we could use. The first major restriction in all CFD applications is the available computational power. For the simulations, the mesh generation and the geometry processing a 6 – core processor with 32 GB of RAM was used in combination with an M2 type SSD Hard Drive.

Although k-omega and SST models are highly recommended for external flows, the mesh requirements are of high standards. In the case where the CAD model of the car corresponds to the real car's dimensions, the flow domain is very large hence such a fine mesh would be consisted of about 80 to 100 million cells. The computational effort to solve the fluid flow is prohibitive. As a result, the three types of k-epsilon models were employed. [3]

From the three available models, k-epsilon Standard, RNG and Realizable, only the last one managed to give a converged solution with stable aerodynamic coefficients for enough iterations. The other two models presented high fluctuations and eventually diverged. So after some simulations which tested their capabilities, we chose the k-epsilon Realizable turbulence model.

D. The k-epsilon Realizable model

It is one of the most commonly used models. Equations for representing the turbulent properties of the flow and resolve effects of convection and diffusion of turbulent energy, are used. It is a two equation model which employs the transport equations of kinetic energy and turbulent dissipation rate. The k-epsilon Realizable model utilizes:

- A new eddy-viscosity formula involving a variable Cμ originally proposed by Reynolds.
- A new model equation for dissipation based on the dynamic equation of the mean square velocity fluctuation.

With this method it is more likely to achieve accurate results of Cd and Cl within a range of 2 – 7% of the real car's coefficient values. Moreover, it is considered to be a stable turbulence model with fast convergence. [4]

E. Wall functions

The fact that there is a thin layer of fluid (viscous sublayer) very close to the wall before the flow becomes fully turbulent (logarithmic region of velocity) leads to rapid variation of the fluid's viscosity as the distance from the wall increases. As a result, the shear stress through the boundary layer cannot be correctly calculated by the velocity difference at each position (height from the wall) by using the mean viscosity. Therefore, arises the necessity of using methods for approaching the flux near the solid boundary. To model the flow in the layer near the wall we use empirical formulas that provide boundary conditions near the wall for the mean flow and turbulence equations. These formulas and the whole approach process have been in place since 1967 by Patankar and Spalding and are called "Wall Functions". [5]

In fluid mechanics we know that the viscous sublayer corresponds to values of y+ between 0 and 1. Also, they can never exceed 4 to 5. From 5 to 30 we have the buffer layer where turbulent motion is presented and from 30 to 300 there is the fully turbulent region of the boundary layer. In ANSYS Fluent there is an adoption that equations for viscous sublayer are employed for values of y+ below 11.226 while equations of the turbulent region are deployed for values of y+ greater than 11.226. The transitional region is not taken into account. The only way to avoid these assumption is to fully resolve the boundary layer with a very fine mesh.

In our case we make use of "Scalable Wall Functions". The purpose of scalable wall functions is to avoid the problem of improving the mesh near the wall that cancels their standard function. This is done automatically by ensuring that the distance near the wall used by the standard function of this approach is not less than that resulting from the intersection of the linear and logarithmic profiles of velocity.

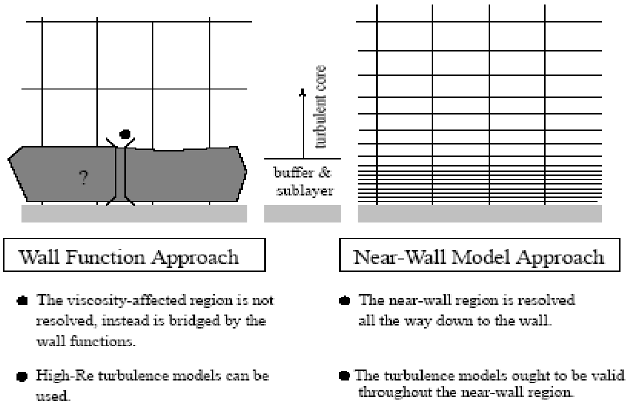

Fig. 1. Near-Wall Treatments in ANSYS FLUENT

F. *Types of algorithms*

The final investigation of Fluent parameters we will use, is the algorithm by which the governing equations are distinguished. From the algorithms that Fluent provides, we have tested the following three: SIMPLE, SIMPLEC and Coupled. The SIMPLE and SIMPLEC algorithms use a relationship between the corrected velocity and pressure to impose the mass preservation principle on the flow field equations in order to predict the pressure distribution therein.

The only difference lies in the expression used for the flow correction. As in SIMPLE, the correction equation can be written as:

$$J_f = J_f^* + d_f\left(\dot{p}_{c0} - \dot{p}_{cl}\right) \quad (4)$$

However, the factor d_f is redefined as a function of the coefficient:

$$\overline{a_P - \sum\nolimits_{nb} a_{nb}}\,. \quad (5)$$

The use of this modified correction equation has been shown to accelerate convergence to problems where pressure-velocity coupling is the main deterrent to achieve a solution.

The coupled system achieves a strong and efficient single phase implementation for steady state flows, with superior performance compared to systems of differentiated solutions. This linked pressure-based algorithm offers an alternative to the density and pressure-based separation algorithm with SIMPLE-type coupling. The separated pressure-based algorithm solves the momentum and pressure equations separately.

Nevertheless, while the Coupled algorithm could theoretically be a better choice, it has been proven by the solution of the flow field with both Coupled and the other algorithms that is showing strong fluctuations and delays convergence. This is explained by the very complex geometry of the car. The SIMPLEC algorithm responded much better and is ultimately the one we choose for our simulations.

III. PRE – PROCESSING

A. *Car Geometry Modeling*

Before the final simulations are resolved, an appropriate geometry preparation was made in order to generate the finite volume mesh. The car's geometry was simplified making the mesh generation process more efficient. We inserted the CAD model in Solidworks 2016, where:

- external geometry details were removed (exhaust pipes, brakes, side mirrors, bumper grilles and lights)
- air vents were closed
- car's wheels (tire and rims) were replaced by closed profile cylindrical geometries
- sharp edges on all surfaces of the car were smoothed (where this was feasible)

The final surface model was converted into a solid part and imported to ANSYS Fluent Design Modeler. The difference between the original model and the converted one which used in the simulations, is presented in Fig. (2) and Fig. (3).

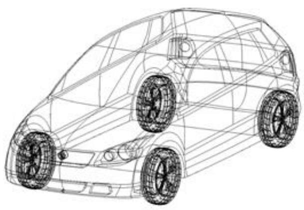

Fig. 2. 3D surface lines of initial geometry

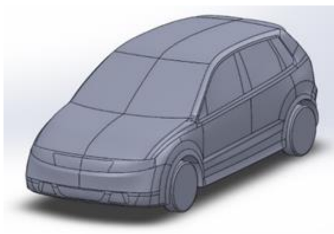

Fig. 3. 3D CAD model view after configuration

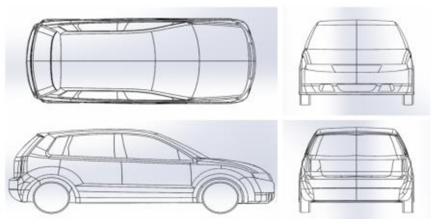

Fig. 4. 2D sketches of car model

The dimensions of the CAD model in comparison with the real one are shown in Table (1).

Table 1. CAD model and real car dimensions

Dimensions (mm)	Real Car*	CAD Model
Length	4149	4593.2
Height	1439	1697.6
Width	1735	1993.7
*Frontal Area: $A = 2.10m^2$		
**Drag Coefficient: $C_d = 0.310$		

In order to have the same Reynolds number for the CAD model and the real car, the model was scaled down by 1.11 (4593.2/4149).

B. *Fluid Domain*

In order to simulate the air flow around the car's body, a control volume needs to be created. The principle of the fluid enclosure is to model a virtual wind tunnel so specifications of modern wind tunnels are taken into account. The first criteria is the distances of the domain boundaries from car's surface. The flow must reach the solid obstacle parallel and undisturbed whereas separation of the boundary layer in the wake region behind the car must be fully developed. The final distances according to car's length are about: 3 Lengths ahead of the car, 5 Lengths after the car, 2 Lengths above and 1 Length from each side [6]. Moreover, a space of 30mm was left between car's wheels and the road. To reduce the overall computational cost and time, the vehicle was considered symmetric about XY plane and only half of the fluid enclose of Fig. (5) was modeled for the simulations.

Last but not least, we checked the blockage ratio to be under 5% as all wind tunnel constructors recommend.

$$Bl = \frac{H \cdot W}{A} = 2.08\% \text{ (<5\%)} \tag{6}$$

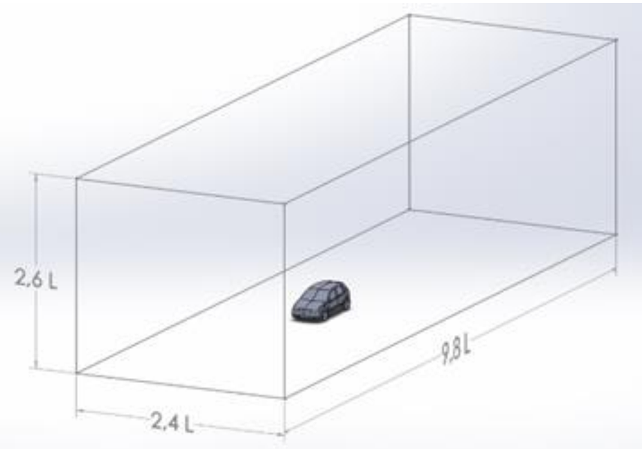

Fig. 5. Fluid domain representing a virtual wind tunnel

C. Accuracy of Wind Tunnel

In order to test the accuracy of the results obtained by constructing the above wind tunnel and the selection of the so far mentioned solver settings, a test case was put under investigation. We used the geometry known as Ahmed Body with a slat angle of 25 degrees and experimental drag coefficient of 0.299. The drag coefficient obtained in this simulation was 0.293 which stands very close to the experimental data for Ahmed body. The results were satisfactory and within the desired accuracy range. [7, 8]

D. Mesh Generation

Meshing process is one of the most important steps of CFD analysis methods. A mesh of improper and/or low quality cells can cause divergence problems to the solution or even lead to unreliable results. It is of high priority to:

- resolve the right region of the boundary layer according to the turbulence model we have chosen
- place enough cells inside the boundary layer
- choose appropriate types of cells for resolving the complexity of the geometry [9]

The mesh that was used is an unstructured mesh of 10 million cells composed by:

- triangular elements at the surface of the car in order to resolve the geometric details accurately
- hexahedral prismatic elements that were extracted from the triangles and placed right after the solid's boundaries to resolve the boundary layer
- and tetrahedral elements which size increases with a rate of 20% as they approach the domain's boundaries

Size functions were used in order to control the size and the quality of the mesh. For the size of the cells in interested regions of the domain, we constructed 3 refinement boxes, one around the car, one at the wake region and one at the underbody of the car. Since boundary layer separation is significant for the drag coefficient, 12 layers of inflation added to the car's surface with a first cell height value of 0.45mm which corresponds to a y+ value of 30. The following figures show the final mesh. [10, 11]

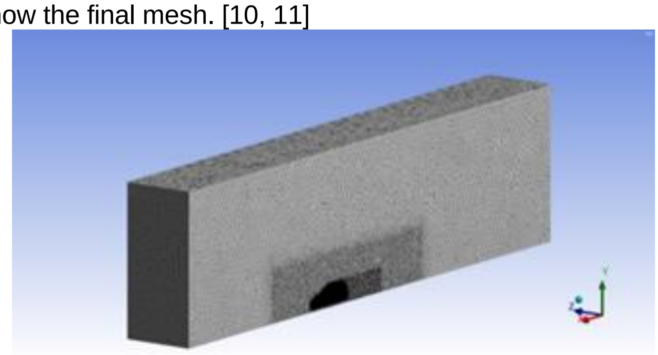

Fig. 6. Mesh generated

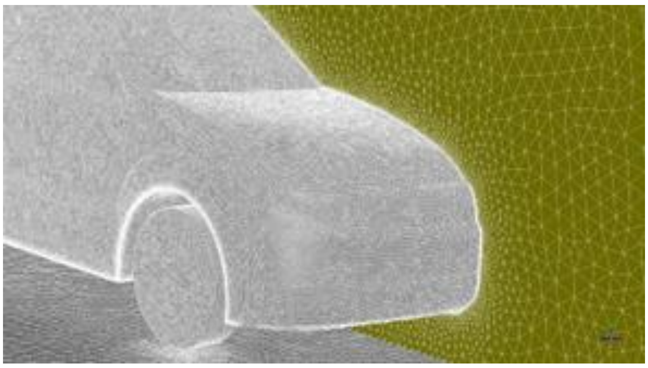

Fig. 7. Detail of mesh on symmetry plane and car surface

E. Mesh Independence Study

Last, a mesh independence study was performed to ensure that the prediction of drag and lift coefficients is reliable no matter the density of the mesh. The study examined 4 meshes with 3, 6, 10 and 16 million cells where not only the density but also the quality of the mesh were increased.

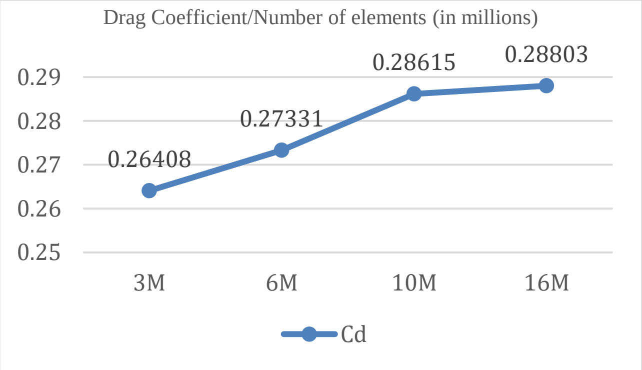

Fig. 8. Drag coefficients vs. mesh density (in millions)

The study indicates that an increasing of density from 10 to 16 million cells does not contribute significantly in the accuracy of the resulted Cd value. As a result, the 10 million mesh is chose for performing the simulations.

Two important criteria for a satisfactory mesh quality are the Orthogonal Quality and Skewness mesh metrics. For the mesh chosen their values are:

- Orthogonal Quality: Minimum=0.1496 Average=0.8804
- Skewness: Maximum=0.8754 Average=0.2306

Minimum Orthogonal Quality must be above 0.10 and maximum skewness values should not surpass 0.90 in order to avoid divergence. [12]

F. Boundary Conditions

The boundary conditions apply to the boundaries of the fluid domain and should approximate the real ones. When the flow enters or exits the computing space, it is necessary to determine some of its characteristics such as velocity and transported turbulence quantities. Fluent provides 10 different types of boundary conditions. We will use two of them. We will apply the threshold velocity inlet to the zone of entry of the wind tunnel and the pressure outlet condition at the exit. From Reynolds number and the characteristic length of the flow, we determine turbulent intensity and length scale as:

$$I \equiv \frac{u'}{u_{avg}} = 0.16 \cdot \left(\mathrm{Re}_{DH}\right)^{-1/8} \Leftrightarrow I = 2.20\% \qquad (7)$$

$$l = 0.07L = 0.29m \qquad (8)$$

Road and Car Body were set as “wall” with no slip condition while the rest of the domain surfaces were set as “symmetry”. [13]

IV. SOLVER SETTINGS OF AIRFLOW

To simulate the conditions of airflow around the car body, a pressure based steady state solver was used. The solver’s settings in Fluent along with the initial conditions and properties of the flow are summarized below:

- Pressure based steady time solver
- k-epsilon Realizable turbulence model with Scalable Wall Functions
- Air at 20^0C with density $\rho = 1.2047\,kg/m^3$ and dynamic viscosity $\mu = 1.8205 \cdot 10^{-5}\,kg/s$ with Reynolds number $\mathrm{Re} = 7.6 \cdot 10^6$
- Velocity $V = 27.78m/s$ (equates 100 km/h) at X-axis direction
- Reference area for calculating lift and drag coefficients set as Frontal Area: $A = 1.25m^2$

Then, the fluid domain was initialized. The initial values of the flow were calculated in all cells by performing a few iterations. This initial guess helps the solution to converge.

In each simulation process of the present paper, the calculations are divided into 3 stages. The first stage is performed in 300 iterations with momentum, turbulent kinetic energy and turbulent dissipation rate set in First Order Upwind to contribute in the convergence of the solution. Then all three sizes are set to Second Order Upwind as this option gives us more accurate final results. Then, the second stage is reached when the Residuals have dropped under 10^{-3}. With a precision granted for all 6 of the residuals below this point, the calculation continues until coefficients of drag and lift have been stabilized for hundreds of iterations for the first 3 decimal places. The stages of the one phase airflow at 100km/h are shown in table (2).

Table 2. Solution stages of one phase airflow at 100km/h

	Stage 1	Stage 2	Stage 3	
Convergence Criteria	10^{-3}	10^{-3}	10^{-6} & stable Cd, Cl	
Iteration Number	300	594	2384	3000
Pressure	Second Order Upwind			
Order of: -Momentum -Kinetic Energy -Dissipation Rate	First Order Upwind	Second Order Upwind		
Cd	0.44446	0.39405	0.28602	0.28615
Cl	0.03058	-0.1228	-0.1110	-0.1110

V. SOLUTION RESULTS

This first simulation is very important as it shows how “close” we are to the experiments made by the constructor of the car in the wind tunnel. At first glance, the CFD value of Cd differs from experimental one by 7.74%. Considering the fact that the frontal area of the CAD model also differs from the real’s one, it would be suitable to compare the product $C_d \cdot A$. In this case the deviation between experimental data and CFD results drops to only 1.15%. The results of this first simulation are more than acceptable. They are satisfactory to an extent that we can safely use them as a benchmark for subsequent simulations. The coefficients obtained by the rain simulations and the addition of the aerodynamic component, will be compared with the results of the above simulation.

*The same simulation was performed with air velocity at 140km/h. The results are presented in conclusions of this paper.

VI. MODELIGN OF RAIN WITH THE DPM MODEL

A. Theory

The two-phase flow of air with water droplets is a complex phenomenon, of which all natural mechanisms are not fully understood. It can be considered as an incompressible transport of water droplets, with air as a carrier and droplets as the transported matter. The model that examines the phenomenon is that of the distinct two phase flow. In this the secondary phase is considered dispersed in the main phase and the interacting forces with the surrounding flux are calculated for each particle. So particles are introduced into the flow and then their trajectory is calculated, as well as their interaction with air (mass and momentum transfer). The model also takes into account the influence of turbulence on orbit and particle motion. [14]

The mass transfer from the discrete phase to continuous is calculated in Fluent by examining the mass changes of a particle as it passes through each control volume of the model. The change in mass is calculated by:

$$M = \frac{\Delta m_p}{m_{p,0}} \dot{m}_{p,0} \tag{9}$$

where:

Δm_p: change in particle mass in the control volume

$m_{p,0}$: the initial mass of the particle

$\dot{m}_{p,0}$: the initial mass flow rate of the particles

This mass exchange appears as a mass source in the continuous phase equation but also as the source of a chemical species that we define. Mass sources are included in all subsequent continuous-phase calculations.

B. Setting up the DPM in Fluent

In order to simulate the rain in Fluent the Discrete Phase Model (DPM) was turned on. Fluent allows the simulation of a second discrete phase in a Lagrange reference frame. This second phase consists of spherical particles (which can be considered droplets or bubbles) dispersed in the continuous phase. Fluent calculates the paths of discrete phase particles as well as the heat and mass transfer between the two phases. The coupling between the phases and its effect on the discrete phase can be included. Fluent provides the following discrete phase configuration options:

- Calculate the path of the discrete flow using Lagrange equations that includes discrete phase inertia, aerodynamic resistance of particles and gravitational force for constant flows.
- Prediction of the effects of turbulence due to turbulent flow in the discrete phase.

To ensure that the above physical mechanisms of the flow will be taken into account for the simulations of rain, we had to activate some specific features of DPM. First of all gravity acceleration was included with a value of $9.82 m/s^2$. The Particle Volume Faction defined as the mass flow of water droplets to the airflow mass, remained below 10% so the equations of DPM model still apply. Based on the dynamic balance of the particles of the discrete phase and their mass and momentum transfer with the continuous phase, the droplet path was calculated by the activation of:

- “Interaction with Continuous Phase”
- “Discrete Random Walk” model
- and the choice “Eddy Lifetime”

The modeling of particle’s behavior inside the flow domain was performed by the “Taylor Analogy Breakup” model (TAB) which includes the deformation of particles, the separation mechanism at contact with the solid surface of the car and the number, volume, shape and velocity of the child droplets after the impact. Moreover, the variation of drag coefficient of droplets is calculated by activating the “Dynamic Drag Model”.

To monitor and observe the paths of the water droplets, Fluent provides the choice of the “Stochastic Track Model” which employs the mean velocity of the continuous phase on the particle trajectories. Moreover, the momently value of velocity was included to predict the dispersion of particles because of turbulence. [15]

C. Boundary and Initial Conditions for Two Phase Flow

The particles insert the fluid domain from a surface parallel to the velocity inlet (XY plane). It is recommended that the two phase flow reaches the obstacle parallel and undisturbed so the surface is placed 5m before the car where the flow meats freestream conditions. The initial conditions for the inserting droplets are the velocity of air at X-direction (27.78m/s in case of 100km/h) and terminal velocity $w_s = -5.2 m/s$ at Y-direction. For calculating the terminal velocity the Eq. (10) was solved by employing an iterative computational method.

$$W = F_b + D \tag{10}$$

where:

W : weight of the particle

F_b : buoyancy force acting on particle

D : drag force acting on particle

With the impact of droplets on car's surface, a water film is created. As a result the roughness of the surface increases and so does the generated drag force. To model this phenomenon the boundary condition "Wall Film" at DPM tab is chosen only for the vehicle's surface. The road was set as "Trapped" while the rest boundaries of the fluid domain were set as "Escaped".

The LWC (Liquid Water Content) is $30 g/m^3$ which corresponds to a mass flow rate of water particles approximately 15kg/s while the mass flow rate of air is 1800kg/s. This gives us a Particle Volume Fraction of 0.83%. [16]

VII. AERODYNAMIC COMPONENT DESIGN

A. *General principles*

The general purpose of using aerodynamic geometric features on a car, is to improve the negative lift coefficient and reduce drag force effects as the car moves through air. For achieving this, the flow must be shaped so that the boundary layer detachment areas are smaller, the turbulence flow disorders and fluctuations become as small as possible and the reverse flow areas occupy less space (especially in the wake region) with the vehicle escaping those areas faster.

B. *Airfoils on cars*

In the present paper, an airfoil was chosen in order to improve the aerodynamic performance of the car in both one phase and two phase flow conditions. The main function of an airfoil is the diffusion of the air passing over the vehicle. This diffusion is achieved by increasing swirling amounts that flow over the car's surface leading to "destroying" the laminar flow and providing a "cushion" for the laminar layer as the air passes through the car's airfoil. Moreover we aim to increase the total vertical force acting on the car. This would function positively to the adhesion of the car, which in rainy conditions and especially in turns, is prone to oversteering effects. These phenomena in all conventional cars are particularly dangerous as they often lead to driver's loss of control of the car. So this is a choice of both improving the performance of the car, but also providing greater security with a more stable car in conditions of heavy rainfall. [17]

C. *NACA – type airfoil*

The airfoil used for the next simulations is a 4 – digit NACA 4312 airfoil with:

- chord length: 150mm
- width: 1400mm
- angle of attack: 15^o

2D design and 3D CAD model are shown in Fig. (9) and Fig. (10), respectively.

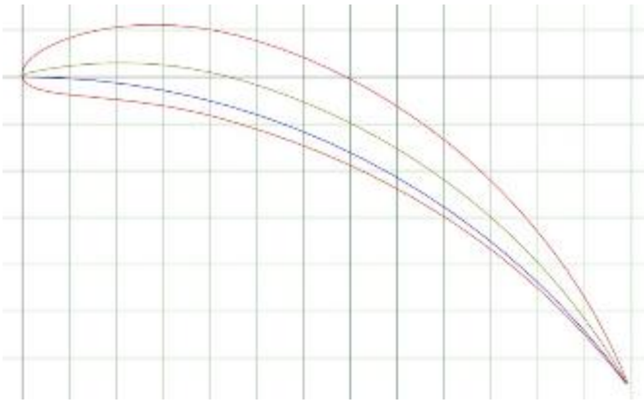

Fig. 9. NACA 4312 sketch design

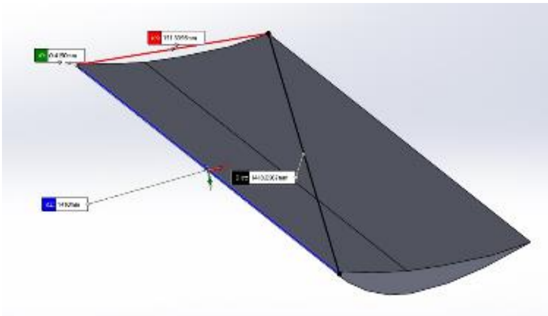

Fig. 10. NACA 4312 CAD model with dimensions

Moreover, the mesh was reconstructed by creating a fine and very detailed representation of the airfoil in ICEM with a corresponding increase in cells from about 10 million cells to 12.

Simulations of the car with the addition of the airfoil were performed both in one phase airflow and two phase flow of air/water in form of rain and in velocities of 100km/h and 140km/h.

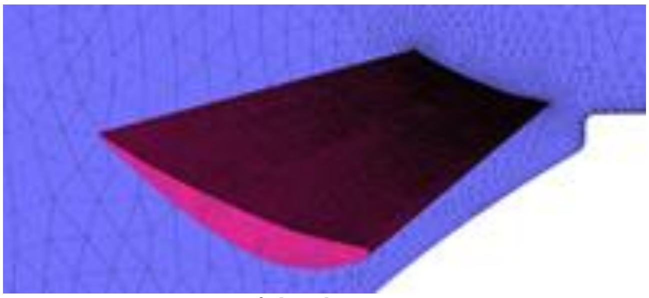

Fig. 11. Airfoil mesh in ICEM

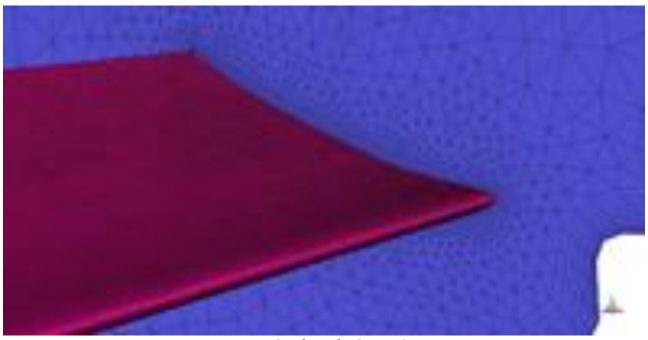

Fig. 12. Detail of airfoil mesh

VIII. POST – PROCESSING AND VISUALIZATION OF THE FLOW

From the steady state analysis of the flow field both at air and rain conditions with and without the airfoil, as well as in velocities of 100km/h and 140km/h, final values of drag and lift coefficients were obtained. The variations of Cd and Cl are shown in Tables (3) and Table (4).

*The one phase airflow coefficients are the only ones compared with the experimental results. The coefficients obtained from the rest of the simulations are compared with those of the one phase airflow at 100km/h.

Table 3. Drag coefficient results

	Drag Coefficient Cd			
speed	One phase airflow		Two phase flow (rain)	
(km/h)	Car	Car+airfoil	Car	Car+airfoil
100	0.286	0.310	0.293	0.329
140	0.304	0.351	0.315	0.381

Table 4. Lift coefficient results

	Lift Coefficient Cl			
speed	One phase airflow		Two phase flow (rain)	
(km/h)	Car	Car+airfoil	Car	Car+airfoil
100	-0.111	-0.148	-0.106	-0.146
140	-0.139	-0.181	-0.131	-0.180

From the tables above we can conclude that:

- ✓ The addition of the airfoil caused an increasing of drag by 8.39% while the absolute negative lift (downforce) increased by 33.33%
- ✓ Rain caused an increasing of drag by 2.45% and a degradation of lift coefficient by 4.72%
- ✓ The addition of the airfoil in conditions of heavy rainfall increased drag coefficient by 12.29% while negative lift coefficient was increased by 37.74%

Similar results were obtained by the simulations of 140km/h but with the intense of the flow turbulence fluctuations being much higher cause of the higher flow's Reynolds number.

In the next pages there are presented the visualized results of the CFD analysis in forms of contours and streamlines. They help us visualize the actual flow behavior. It is a useful tool to understand and analyze how the flow field is formed around the car in order to make the appropriate improvements.

All Figures are for velocities of 100km/h.

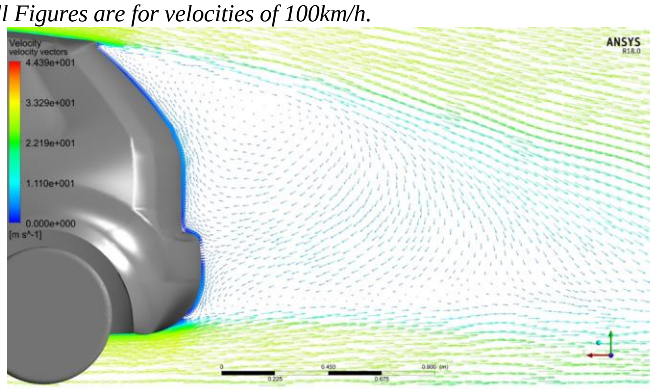

Fig. 13. Velocity vectors in wake region behind the car

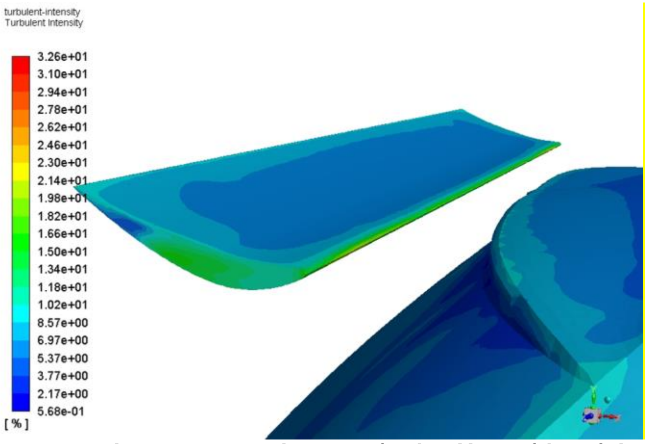

Fig. 14. Velocity vectors in wake region after the addition of the airfoil

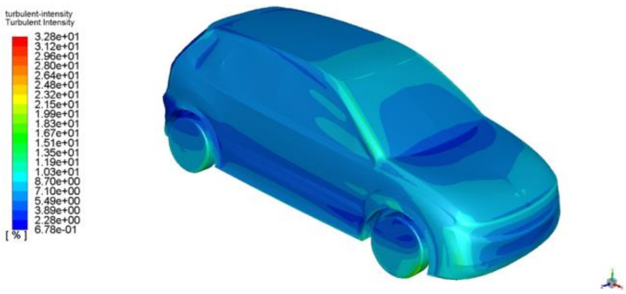

Fig. 15. Turbulent intensity over the car body

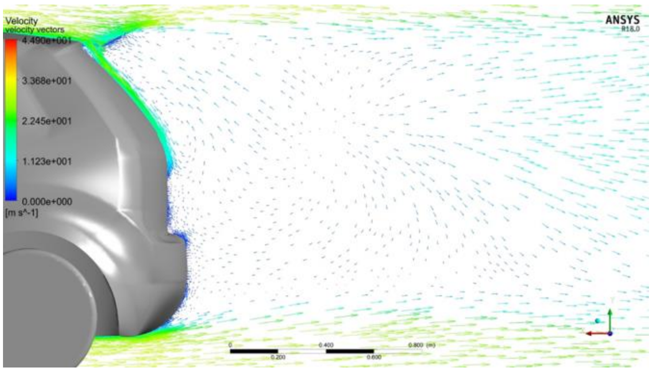

Fig. 16. Turbulent intensity over the airfoil

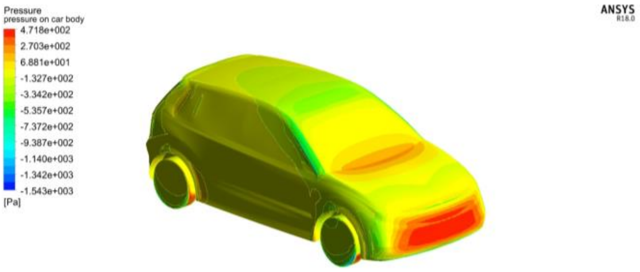

Fig. 17. Pressure contour on car body

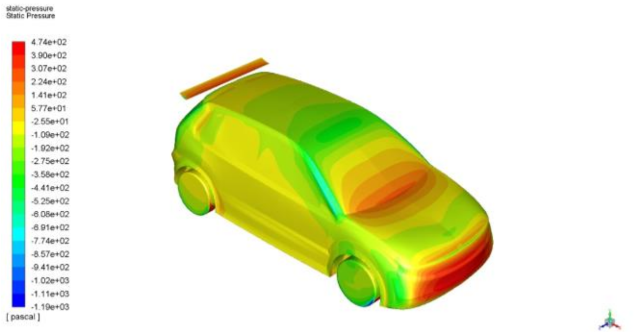

Fig. 18. Pressure contour on car body with airfoil

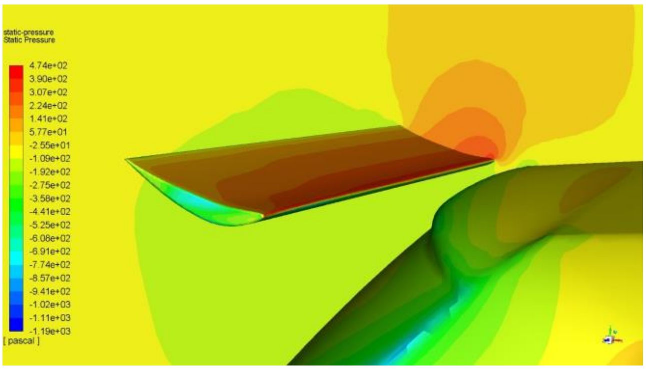

Fig. 19. Pressure contour on airfoil

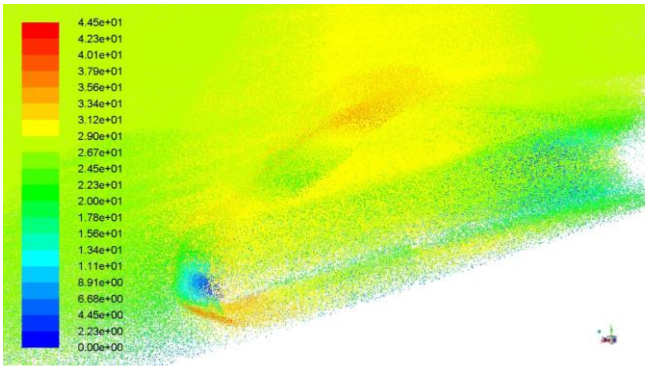

Fig. 20. Rain droplets distribution around the car

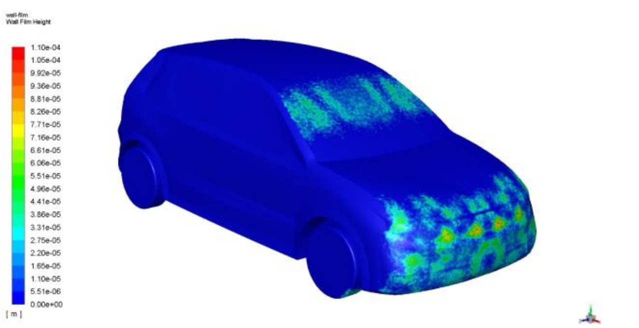

Fig. 21. Wall film height distribution on car surface

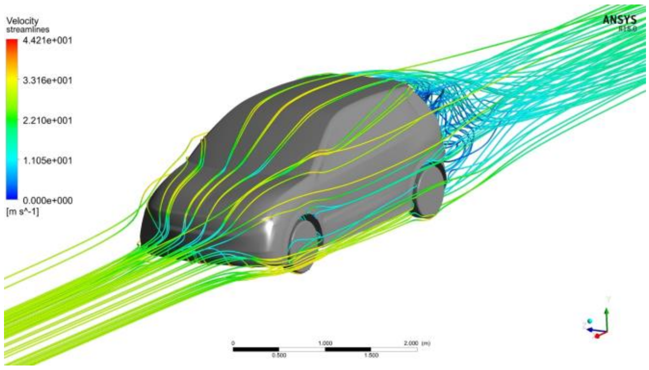

Fig. 22. Velocity streamlines around car body

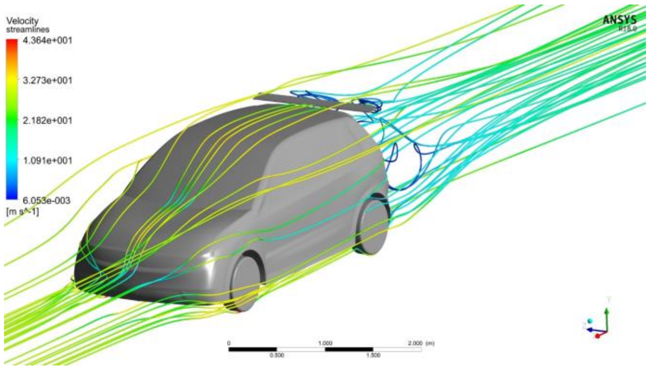

Fig. 23. Velocity streamlines around car body with airfoil

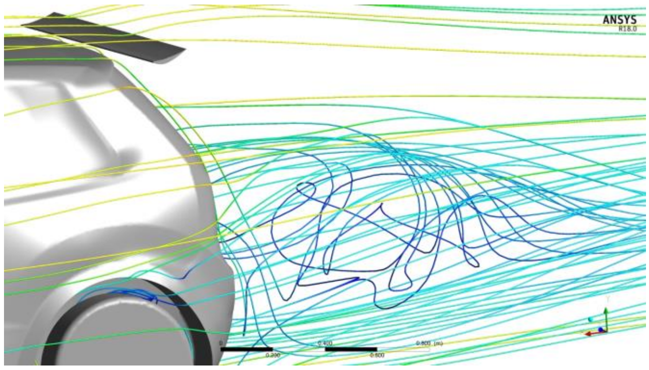

Fig. 24. Velocity streamlines in wake region for car with airfoil

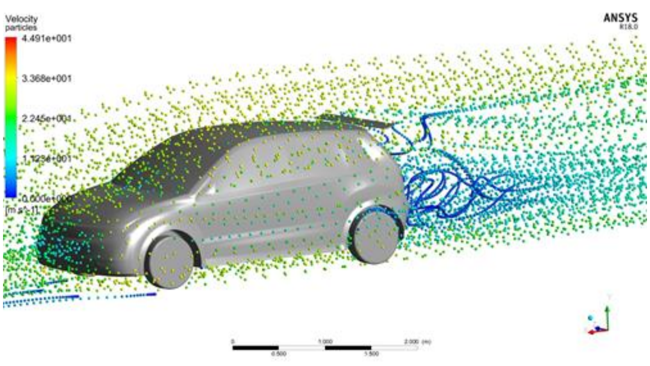

Fig. 25. Air particles distribution around car body

Fig. 26. Static pressure contour

Fig. 27. Static pressure contour around car with airfoil added

Fig. 28. Detail of static pressure contour around the airfoil

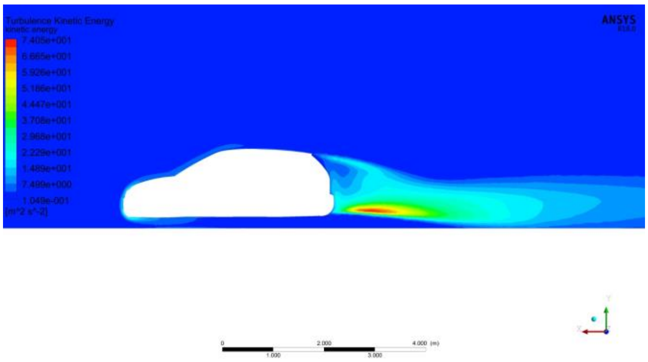

Fig. 29. Turbulence kinetic energy contour

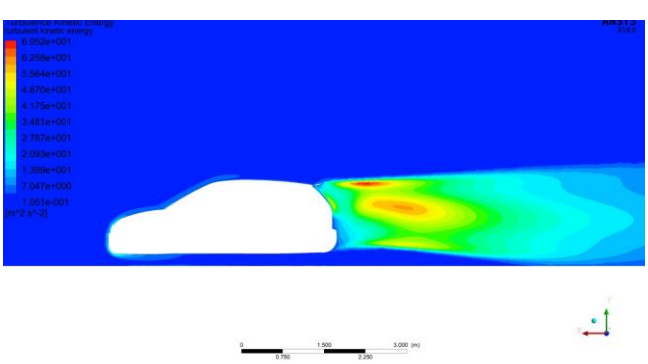

Fig. 30. Turbulence kinetic energy around car with airfoil added

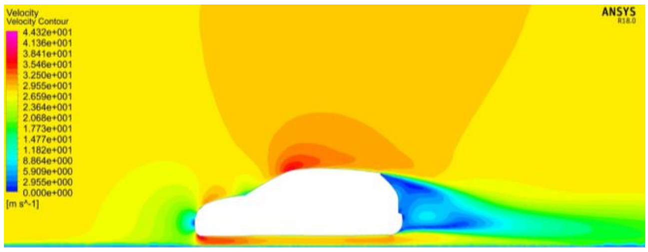

Fig. 31. Velocity contour

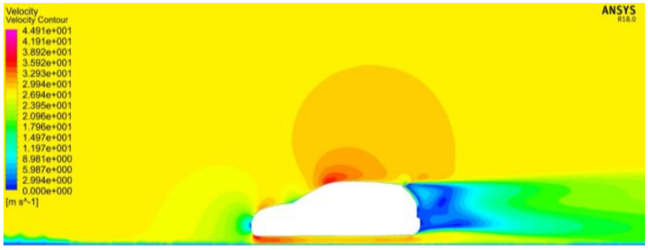

Fig. 32. Velocity contour around car with airfoil added

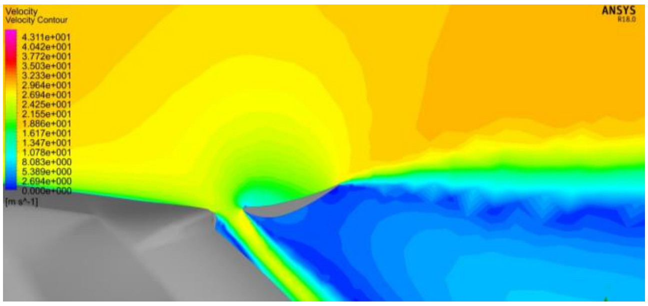

Fig. 33. Detail of velocity contour around the airfoil

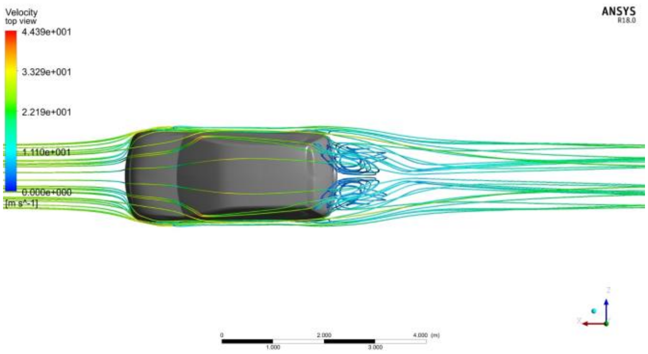

Fig. 34. Velocity streamlines from top view

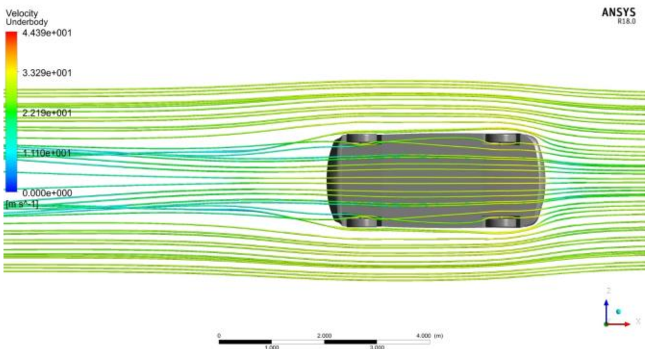

Fig. 35. Velocity streamlines at the underbody

The results obtained can be summarized as:

- Drag is increased by the addition of the airfoil but with additional resistance appearing on the car body instead of the spoiler. This can be explained by how the spoiler reshapes the air flow path at the wake region. The flow pattern at that point causes the increased disorder in such a way that the reverse flow area produces substantially greater resistance. This observation also appears in the contours of pressure and kinetic energy that follow in a next section of this paper.

- The percentage and absolute value increase of downforce is very large in relation to the total vertical force acting on the car without the spoiler. This makes the spoiler a highly efficient option for our purpose, which is to increase the car's stability in single-phase and two-phase flow.

- In severe rains, the vertical force (negative lift) decreases as the lift coefficient is degraded while at the same time there is little increase in the drag force. Overall, the aerodynamic behavior of the car tends to the worst as the power required to overcome the car viscous and inertial flow forces is increased while the force that determines its stability is reduced.

- The effect of rain on aerodynamic resistance is relatively small. At higher speeds or in high performance cars and racing cars, it may have a greater impact or even these small changes might play a more decisive role in the performance of the car. In these cases, the study of aerodynamic elements that can improve the performance of the car and especially in heavy rains, will be even more important.

IX. CONCLUSION

The use of the airfoil is not only for the additional vertical force for the stability of the car, but also for the rear flow reform so that the reverse flow area is smaller and at the same time the car's speed of escape from this area is greater. Essentially, we aim to direct the flow in such a way that the "trace" left by the car's motion against the ideal still air, moves away from the car as far possible in the shortest time. This as a general principle can balance to some extent the effect of the aerodynamic element on the vehicle's overall drag coefficient and to make the spoiler more efficient. The velocity and kinetic energy distribution diagrams show the above. The reverse flow area has more intense features at a greater distance from the car's rear end.

From the perspective of computational results accuracy and credibility, we are satisfied because although the finite volume mesh was developed by resolving only the turbulent region of the boundary layer and a RANS model was used, the process of predicting the backflow regions, the detachment of the boundary layer, the separating points and the pressure and velocity distributions on car and airfoil, have been performed with enough precision.

REFERENCES

[1] Margaris D.E., "Two-phase flow in ducts and boundary layers", University of Patras, Patras, 2015

[2] Angelos Th. Papaioannou, "FLUID MECHANICS", 2nd Edition, VOLUME II

[3] ANSYS Inc. “Turbulence Modeling. Introduction to ANSYS Fluent” February 2014

[4] ANSYS Inc. “Introductory FLUENT Training Solver Settings and Modeling Turbulent Flows” version 6.3 December 2006

[5] Launder, B.E., Spalding, "The numerical computation of turbulent flows". Computer Methods in Applied Mechanics and Engineering, March 1974

[6] Darko Damjanović, Dražan Kozak, Marija Živić, Željko Ivandić, Tomislav Baškarić, “CFD analysis of concept car in order to improve aerodynamics”, Mechanical Engineering Faculty in Slavonski Brod, Josip Juraj Strossmayer, University of Osijek

[7] S.R. Ahmed, G. Ramm, “Some Salient Features of the Time-Averaged Ground Vehicle Wake”, SAE-Paper 840300, 1984

[8] W. Meile1, G. Brenn1 “Experiments and numerical simulations on the aerodynamics of the Ahmed body”, Institute of Fluid Mechanics and Heat Transfer (ISW), Graz University of Technology

[9] Abhishek Khare, Ashish Singh, Kishor Nokam, “Best Practices in Grid Generation for CFD Applications Using HyperMesh”, Computational Research Laboratories

[10] Marco Lanfrit, “Best practice guidelines for handling Automotive External Aerodynamics with FLUENT”, Version 1.2, Feb 9th 2005

[11] OZEN ENGINEERING Inc, “Meshing Workshop”, November 2014

[12] ANSYS Inc. “ANSYS Meshing Advanced Techniques” April 2017

[13] Akshay Parab, Ammar Sakarwala, Bhushan Paste, Vaibhav Patil, “Aerodynamic Analysis of a Car Model using Fluent-Ansys 14.5” Department of Mechanical Engineering Rajiv Gandhi, Institute of Technology Mumbai, India

[14] ANSYS Fluent inc. “Chapter 19. Discrete Phase Models” December 2001

[15] ANSYS inc. “Multiphase Modelling in Automobile Industries” 2012

[16] Doubi Eleni, "Experimental and Computational Investigation of Aerodynamic Behavior of Wings in Two-Phase Air-Water Flow and Application to Wind Turbine Wings", PhD Thesis, Department of Mechanical Engineering and Aeronautics, University of Patras, Patras 2013

[17] Wolf-Heinrich Hucho, “Aerodynamics of Road Vehicles” 1993